

Statistics of polaritons in the nonlinear regime

Paolo Schwendimann

Defense Procurement Agency, System Analysis Division, CH 3003 Bern, Switzerland

Cristiano Ciuti*

Department of Physics, University of California, San Diego, La Jolla, California 92093-0319, USA

Antonio Quattropani

Institute of Theoretical Physics, CH 1015 Lausanne-EPFL, Switzerland

(Received 2 May 2003; revised manuscript received 23 July 2003; published 20 October 2003)

We discuss the quantum statistical properties of exciton polaritons in semiconductor microcavities. The nonlinear dynamics is treated within a model of interacting bosons for the signal, pump, and idler modes. We focus on the regime of parametric amplification below threshold. We present the time evolution of the signal and idler modes towards their stationary solutions and discuss their statistical properties. In particular, we evaluate the amount of squeezing of the radiation emitted out of the microcavity in a configuration, which may be relevant for experiments.

DOI: 10.1103/PhysRevB.68.165324

PACS number(s): 71.36.+c, 73.20.Mf, 73.21.Fg

I. INTRODUCTION

Microcavity polaritons were observed for the first time in 1992 (Ref. 1) and play a central role in understanding the linear optical properties of quantum wells embedded in semiconductor microcavities.² They arise from the strong interaction between exciton and photons inside the microcavity and are two-dimensional quasiparticles with quite exotic properties. Unlike the quantum well excitons, the microcavity polaritons have a very sharp energy dispersion³ due to the cavity photon component, which has a very light mass. Unlike the cavity photons, polaritons have a pronounced nonlinear behavior because of the exciton-exciton interaction and of the anharmonic exciton-photon coupling (saturation). Remarkably, semiconductor microcavities allow us to achieve a two-dimensional system of small mass quasiparticles, which can be manipulated by laser beams both in energy and momentum space.

In the last few years nonlinear optical properties of quantum wells embedded in microcavities have been observed and interpreted in terms of microcavity polariton scattering.^{4,5} In these experiments, an external laser field excites two polaritons (pump polaritons) at the field energy. The pump polaritons are scattered under conservation of energy and momentum into two different polaritons modes, which are called signal and idler modes, respectively. In the experimental configuration⁴ the signal mode is at $\mathbf{q}=0$, which is the lowest energy state. A low intensity probe pulse at $\mathbf{q}=0$ is used in order to test the response of the system. This pulse becomes amplified and the amplification enormously grows as a threshold value of the excitation field intensity is approached. This is the characteristic behavior of a parametric amplifier.

Starting from this result, more features have been demonstrated experimentally.⁶⁻⁸ We mention the observation of amplified polariton luminescence^{4,6} the determination of threshold behavior of the amplifier, where macroscopic polarization states spontaneously appear and the evidence for

multiple scattering effects above threshold.^{6,8} The statistics of the photons emitted by nonlinear systems has been extensively studied in quantum optics. In this context, the parametric amplifier model has played a central role when investigating nonclassical quantum optical effects.⁹ In particular, squeezing of the radiation field has been extensively discussed within this model. The experimental observation of a parametric effect involving polaritons raises the question, whether any statistical properties of the polaritons and in particular squeezing could be observable in this system. Indeed, it has been pointed out^{10,11} that bulk polariton states have some intrinsic statistical properties and in particular, they exhibit squeezing, although no important squeezing is expected in the linear regime both in the bulk case and for microcavity polaritons.^{10,12} On the contrary, generation of nonclassical light is promising in the nonlinear regime.¹³⁻¹⁶ Polaritons are half-light half-matter excitations, hence a measurement of the field emitted from microcavity will give direct access to the statistical properties of the polaritons matter inside the cavity. Thus, it will allow us to investigate new and interesting properties of the polariton matter. In this paper we discuss the statistical properties of the polariton amplifier without a probe. We will refer to the experimental configuration introduced to observe amplified photoluminescence⁵ and consider a simplified three mode model, which has already been successfully used in discussing the parametric amplification and luminescence of polaritons.¹⁷⁻²⁰ As is well known a threshold characterizes the parametric system, below which a small injected signal is amplified and above which the system behaves similar to a nonlinear oscillator. The model considered in this paper allows a satisfactory description of the nonlinear effects below the threshold. Above threshold more polariton modes are involved in the dynamics and have to be included in the model.^{6,19} In a first step we investigate the dynamics of the system in the regime of continuous pumping below threshold. In particular we discuss the time evolution of the polariton operators around the stationary value of the pump mode

and the dynamics of the signal and idler population as well as of the anomalous correlation (the expectation value of the product of the signal and idler amplitudes). We find that the signal and idler modes are strongly correlated during the whole time evolution. In a second step we discuss the correlations in the polariton system in the stationary regime. We characterize the behavior of the system at the parametric threshold and give the expression for the first order and second order correlations from which the basic information on the polariton statistics can be obtained. In particular we concentrate on squeezing, whose magnitude is shown to be comparable with the one obtained from the quantum optical models. Recently, the measurement of squeezing in a configuration corresponding to a degenerate polariton parametric amplifier has been discussed.²¹ We present results on spectral squeezing for this system as an application of the considerations developed above. The model is presented in Sec. II. In Secs. III and IV the dynamics and the stationary solutions are discussed. Section V is devoted to the polariton statistics and squeezing in the nondegenerate amplifier whereas squeezing in the degenerate amplifier is discussed in Sec. VI.

II. MODEL

Polaritons in a microcavity are resonantly excited by a laser field well below the saturation limit for the excitons. As it is well known, polaritons behave as bosons in the low excitation limit. The bosonic behavior survives as long as the exciton density is much smaller than the typical exciton saturation density.²² Therefore, it is possible to discuss the optical properties of interacting polaritons in terms of interacting bosons.¹⁸ This property allows simple modeling of the main features of the polariton amplification process, which is a consequence of polariton-polariton scattering. In the following we consider the polariton to be bosons.^{17,18}

Polariton-polariton scattering involves polariton pairs, whose wave vectors take all the values allowed by momentum conservation. Here we consider only the energy and momentum conserving interaction between three polariton modes: the pump mode \mathbf{k} , the signal mode at \mathbf{q} , and the idler mode at $(2\mathbf{k}-\mathbf{q})$. This is justified because polaritons are excited resonantly at a fixed \mathbf{k} and we restrict the discussion to the parametric amplification regime where the contribution of multiple scattering is negligible.^{17,18} Furthermore, we consider a cw excitation and do not apply any probe beam. In this configuration, the scattering process will be triggered by the quantum fluctuations in the system. The Hamiltonian for the interacting polaritons reads¹⁷

$$H = H_{LP} + H_{PP}^{\text{eff}}. \quad (1)$$

The free term $H_{LP} = \sum_{\mathbf{q}} \hbar \omega_{LP}(\mathbf{q}) p_{\mathbf{q}}^+ p_{\mathbf{q}}$ contains the lower polariton energy dispersion $\omega_{LP}(\mathbf{q})$ and $p_{\mathbf{q}}, p_{\mathbf{q}}^+$ are the annihilation and creation Bose polariton operators defined as $p_{\mathbf{q}} = X_{\mathbf{q}} b_{\mathbf{q}} + C_{\mathbf{q}} a_{\mathbf{q}}$, where $b_{\mathbf{q}}, a_{\mathbf{q}}$ are the exciton and photon Bose operators, respectively, and $X_{\mathbf{q}}, C_{\mathbf{q}}$ ($X_{\mathbf{q}} > 0$ and $C_{\mathbf{q}} < 0$) are the corresponding Hopfield coefficients.¹⁷ The effective interaction Hamiltonian in Eq. (1) describes scattering processes between pairs of polariton operators with mo-

mentum conservation and is presented and discussed in Refs. 17, 18. As already stated above we will restrain ourselves to consider only scattering processes involving three polariton modes. In the following we consider the modes $\mathbf{q}=0$ (signal), \mathbf{k} (pump), $2\mathbf{k}$ (idler). The polariton-polariton interaction terms read

$$H_{PP}^{\text{eff}} = \hbar \omega_{\text{int}} p_{2\mathbf{k}}^+ p_0^+ p_{\mathbf{k}} p_{\mathbf{k}} + \text{H.c.} \quad (2)$$

Notice that ω_{int} is positive and represent a repulsive interaction. Its explicit form is reported in Refs. 17–19. It contains the contributions of the exciton-exciton interaction and of the exciton saturation. This Hamiltonian describes the interaction between polaritons in a loss less cavity. In practice, the quantum well is embedded in a microcavity whose mirrors are distributed Bragg reflectors. These have a non-negligible transmission coefficient, which is a source of losses. In order to account for these losses and for the interaction with the external laser field for simplicity we work within the well-known quasimode approximation.² The quasimode Hamiltonian takes the form

$$H_{\text{qm}}(\mathbf{q}) = \int d\Omega \{v(\Omega) C_{\mathbf{q}} p_{\mathbf{q}}^+ \alpha_{\mathbf{q},\Omega} + \text{H.c.}\}, \quad (3)$$

where $v(\Omega)$ is the frequency-dependent reflectivity of the stop band of the microcavity. The identification of the coupling coefficient in Eq. (4) with the reflectivity is a fundamental feature of the quasimode approach.² The operator $\alpha_{\mathbf{q},\Omega}$ destroys an external photon with in-plane momentum \mathbf{q} and a generic frequency Ω . The external source field is coupled to the polaritons through the Hamiltonian

$$H_{\text{pump}} = \hbar F_{\text{pump}}(t) p_{\mathbf{k}}^+ + \text{H.c.} = \hbar F_{\text{pump}} \exp[i\omega_{\text{pump}} t] p_{\mathbf{k}}^+ + \text{H.c.} \quad (4)$$

The Heisenberg equations of motion for the three polariton operators are straightforwardly obtained from Eqs. (1), (3), and (4). In order to describe dissipation, we perform the standard elimination of the external field dynamics. This procedure allows us to introduce the lifetimes $\gamma_0, \gamma_{\mathbf{k}}, \gamma_{2\mathbf{k}}$, of the polariton modes and the corresponding Langevin force operators $\mathbf{F}_0(t), \mathbf{F}_{\mathbf{k}}(t), \mathbf{F}_{2\mathbf{k}}(t)$, which are defined as

$$\mathbf{F}_{\mathbf{q}}(t) = \int d\Omega v(\Omega) C_{\mathbf{q}} \alpha_{\mathbf{q},\Omega}(t=0) \exp[-i\Omega t]. \quad (5)$$

The Langevin equation for the polariton modes read

$$i \frac{d}{dt} p_0(t) = [\tilde{\omega}_{LP}(0) - i\gamma_0] p_0(t) + \omega_{\text{int}} \hat{p}_{\mathbf{k}}^2(t) \hat{p}_{2\mathbf{k}}^+(t) + \mathbf{F}_0(t), \quad (6a)$$

$$i \frac{d}{dt} \hat{p}_{2\mathbf{k}}^+(t) = [2\omega_{\text{pump}} - \tilde{\omega}_{LP}(2\mathbf{k}) - i\gamma_{2\mathbf{k}}] \hat{p}_{2\mathbf{k}}^+(t) - \omega_{\text{int}} \hat{p}_{\mathbf{k}}^{+2}(t) p_0(t) - \mathbf{F}_{2\mathbf{k}}^*(t) e^{-i2\omega_{\text{pump}} t}, \quad (6b)$$

$$\begin{aligned}
 i\hbar \frac{d}{dt} \hat{p}_{\mathbf{k}}(t) = & [\tilde{\omega}_{\text{LP}}(\mathbf{k}) - \omega_{\text{pump}} + i\gamma_{\mathbf{k}}] \hat{p}_{\mathbf{k}}(t) \\
 & + 2\omega_{\text{int}} \hat{p}_{\mathbf{k}}^+(t) p_0(t) \hat{p}_{2\mathbf{k}}(t) + \mathbf{F}_{\mathbf{k}}(t) e^{-i\omega_{\text{pump}}t} \\
 & + F_{\text{pump}}(0), \tag{6c}
 \end{aligned}$$

where $F_{\text{pump}}(t) = F_{\text{pump}}(0) e^{i\omega_{\text{pump}}t}$, $p_{2\mathbf{k}}(t) = p_{2\mathbf{k}}(t) e^{i2\omega_{\text{pump}}t}$, $p_{\mathbf{k}}(t) = \hat{p}_{\mathbf{k}}(t) e^{i\omega_{\text{pump}}t}$.

In Eq. (6), we have introduced the renormalized polariton frequencies $\tilde{\omega}_{\text{LP}}(\mathbf{q})$ defined below, $\tilde{\omega}_{\text{LP}}(\mathbf{q})$ is blueshifted with respect to the unperturbed lower polariton frequency $\omega_{\text{LP}}(\mathbf{q})$, because of the repulsive polariton-polariton interaction.¹⁷ Since we are describing an irreversible process, the equation of motion verified by $p_0^+(t)$ contains the term $i\gamma_0$ with the same sign as in $p_0(t)$. The commutation relations are granted by the presence of the Langevin force operators $\mathbf{F}_0(t)$, $\mathbf{F}_{\mathbf{k}}(t)$, $\mathbf{F}_{2\mathbf{k}}(t)$.

III. TIME DEPENDENT SOLUTION

In order to understand the dynamics of the population transfer between pump mode and signal and idler modes, we have to discuss the dynamics of the polariton amplifier. In particular, we are interested in the behavior of the system in the vicinity of the parametric threshold. In principle, this information is contained in the Eq. (6). However, the operator equations (6) cannot be solved in this form as they involve products of three oscillator operators. A simplification is achieved by noticing that the pump mode $p_{\mathbf{k}}$ is coupled to a macroscopic stationary external field (the exciting laser field). Through this coupling, the polariton state \mathbf{k} acquires a macroscopic amplitude.

We account for this feature by replacing the pump polariton operator $p_{\mathbf{k}}(t)$ by its expectation value $P_{\mathbf{k}}(t) \equiv \langle \hat{p}_{\mathbf{k}} \rangle \times(t)$. In this case the equation of motion of the pump mode (6c) for resonant excitation, i.e., $\tilde{\omega}_{\text{LP}}(\mathbf{k}) = \omega_{\text{pump}}$ reads

$$i \frac{dP_{\mathbf{k}}(t)}{dt} = -i\gamma_{\mathbf{k}} P_{\mathbf{k}}(t) + 2\omega_{\text{int}} P_{\mathbf{k}}^*(t) \langle p_0 \hat{p}_{2\mathbf{k}} \rangle(t) + F_{\text{pump}}(0). \tag{7}$$

In this last expression, the mean value $\langle \hat{p}_{\mathbf{k}}^+ p_0 \hat{p}_{2\mathbf{k}} \rangle$ has been factorized into the product of mean values $\langle \hat{p}_{\mathbf{k}}^+ \rangle(t) \langle p_0 \hat{p}_{2\mathbf{k}} \rangle \times(t) = P_{\mathbf{k}}^*(t) \langle p_0 \hat{p}_{2\mathbf{k}} \rangle(t)$. This approximation is justified because the pumped mode is macroscopically occupied, whereas the signal and idler modes are not. Within this approximation we finally obtain the equations of motion for the signal and idler operators

$$i \frac{d}{dt} p_0(t) = [\tilde{\omega}_{\text{LP}}(0) - i\gamma_0] p_0(t) + \omega_{\text{int}} P_{\mathbf{k}}^2(t) p_{2\mathbf{k}}^+(t) + \mathbf{F}_0(t), \tag{8a}$$

$$\begin{aligned}
 i \frac{d}{dt} \hat{p}_{2\mathbf{k}}^+(t) = & [2\omega_{\text{pump}} - \tilde{\omega}_{\text{LP}}(2\mathbf{k}) - i\gamma_{2\mathbf{k}}] \hat{p}_{2\mathbf{k}}^+(t) \\
 & - \omega_{\text{int}} P_{\mathbf{k}}^{*2}(t) p_0(t) - \tilde{\mathbf{F}}_{2\mathbf{k}}^+(t). \tag{8b}
 \end{aligned}$$

Here $\tilde{\omega}_{\text{LP}}(\mathbf{q}) = \omega_{\text{LP}}(\mathbf{q}) + 2\omega_{\text{int}} |P_{\mathbf{k}}|^2$ is the renormalized frequency, which includes the blueshift. In order to discuss the dynamics of the polariton interaction, Eqs. (8) have to be solved together with Eq. (7). To this end we construct from Eq. (8) a set of coupled equations for the anomalous correlation $A(t) = \langle p_0 \hat{p}_{2\mathbf{k}} \rangle(t)$ and for the expectation values of the number operators of the polaritons in the signal and idler modes. These equations read

$$i \frac{d}{dt} A(t) = (\omega_T - i\gamma_T) A(t) + \omega_{\text{int}} P_{\mathbf{k}}^2(t) [N_0(t) + N_{2\mathbf{k}}(t) + 1], \tag{9a}$$

$$\begin{aligned}
 i \frac{d}{dt} A^*(t) = & -(\omega_T + i\gamma_T) A^*(t) - \omega_{\text{int}} P_{\mathbf{k}}^{*2}(t) [N_0(t) \\
 & + N_{2\mathbf{k}}(t) + 1], \tag{9b}
 \end{aligned}$$

$$i \frac{d}{dt} N_0(t) = -2i\gamma_0 N_0(t) + \omega_{\text{int}} [P_{\mathbf{k}}^2(t) A^*(t) - P_{\mathbf{k}}^{*2}(t) A(t)], \tag{9c}$$

$$\begin{aligned}
 i \frac{d}{dt} N_{2\mathbf{k}}(t) = & -2i\gamma_{2\mathbf{k}} N_{2\mathbf{k}}(t) + \omega_{\text{int}} [P_{\mathbf{k}}^2(t) A^*(t) \\
 & - P_{\mathbf{k}}^{*2}(t) A(t)], \tag{9d}
 \end{aligned}$$

where

$$\begin{aligned}
 N_0(t) = \langle p_0^+ p_0 \rangle(t), \quad N_{2\mathbf{k}}(t) = \langle \hat{p}_{2\mathbf{k}}^+ \hat{p}_{2\mathbf{k}} \rangle(t), \quad \gamma_T = \gamma_{2\mathbf{k}} \\
 + \gamma_0, \quad \omega_T = \tilde{\omega}_{\text{LP}}(2\mathbf{k}) + \tilde{\omega}_{\text{LP}}(0) - 2\omega_{\text{pump}}. \tag{10}
 \end{aligned}$$

Before discussing the general solution of Eqs. (7) and (9), it is useful to understand the dynamical behavior of the system when the pump mode is in the stationary regime. From Eq. (7) we obtain

$$-i\gamma_{\mathbf{k}} P_{\mathbf{k}} + 2\omega_{\text{int}} P_{\mathbf{k}}^* \langle p_0 \hat{p}_{2\mathbf{k}} \rangle + F_{\text{pump}}(0) = 0. \tag{11}$$

In this last expression, $P_{\mathbf{k}}$, $P_{\mathbf{k}}^*$, and $\langle p_0 \hat{p}_{2\mathbf{k}} \rangle \equiv A^{\text{sat}}$, which represents the phase-dependent anomalous correlation, are stationary quantities. We notice that the solution for the pump mode will depend explicitly on the stationary anomalous correlation A^{sat} between signal and idler modes. In the following, we will consider the pump mode amplitudes $P_{\mathbf{k}}$, $P_{\mathbf{k}}^*$ to be adjustable parameters. In reality, they are a function of the external field amplitude F_{pump} . The relation between these quantities is given by Eq. (11). We will discuss the solution of Eq. (11) later, once the explicit expression for A^{sat} has been calculated.

In the stationary regime of the pump mode, the inhomogeneous operator equations (8) can be solved analytically, e.g., by Laplace transforms. The solutions are characterized by two complex frequencies ω_{\pm} for both p_0 and $\hat{p}_{2\mathbf{k}}^+$ and by ω_{\pm}^C for both p_0^+ and $\hat{p}_{2\mathbf{k}}$ (Refs. 18, 19)

$$\omega_{\pm} = \frac{1}{2} [\tilde{\omega}_{\text{LP}}(0) - \tilde{\omega}_{\text{LP}}(2\mathbf{k}) + 2\omega_{\text{pump}} - i(\gamma_0 + \gamma_{2\mathbf{k}}) \pm \sqrt{\Lambda}], \tag{12a}$$

$$\omega_{\pm}^C = \frac{1}{2} [\tilde{\omega}_{LP}(2\mathbf{k}) - \tilde{\omega}_{LP}(0) - 2\omega_{\text{pump}} - i(\gamma_0 + \gamma_{2\mathbf{k}}) \pm \sqrt{\Lambda^*}] \quad (12b)$$

with

$$\Lambda = \frac{1}{2} \{ [\tilde{\omega}_{LP}(2\mathbf{k}) + \tilde{\omega}_{LP}(0) - 2\omega_{\text{pump}} - i(\gamma_0 + \gamma_{2\mathbf{k}})]^2 - 4\omega_{\text{int}}^2 |P_{\mathbf{k}}|^4 \}. \quad (13)$$

The solution of Eq. (8) is stable provided that the imaginary part of the frequencies (12) is negative. As a function of the pumped mode $P_{\mathbf{k}}$, the imaginary part of the square root of Eq. (13) may be larger than the sum of the polariton broadenings. In this case, the stability condition is not verified. In particular, when the energy and momentum between pump and signal and idler modes are strictly conserved, we have $\tilde{\omega}_{LP}(2\mathbf{k}) + \tilde{\omega}_{LP}(0) - 2\omega_{\text{pump}} = 0$ and the real part of the square root of Eq. (13) vanishes. The imaginary part of ω_{\pm} changes its sign in function of the pump polariton occupation $|P_{\mathbf{k}}|^2$ and vanishes when

$$\gamma_0 \gamma_{2\mathbf{k}} - \omega_{\text{int}}^2 |P_{\mathbf{k}}|^4 = 0. \quad (14)$$

Equation (14) defines the threshold value $|P_{\mathbf{k}}^{\text{threshold}}|^2 = \sqrt{\gamma_0 \gamma_{2\mathbf{k}}} / \omega_{\text{int}}$ for the parametric process above which the solutions of Eq. (8) become unstable. We notice that when Eq. (14) holds, the frequencies (12) become

$$\omega_{+} = \tilde{\omega}_{LP}(0), \quad (15a)$$

$$\omega_{-} = \tilde{\omega}_{LP}(0) - i(\gamma_0 + \gamma_{2\mathbf{k}}), \quad (15b)$$

$$\omega_{+}^C = -\tilde{\omega}_{LP}(0), \quad (15c)$$

$$\omega_{-}^C = -\tilde{\omega}_{LP}(0) - i(\gamma_0 + \gamma_{2\mathbf{k}}). \quad (15d)$$

In this case the frequencies ω_{+} and ω_{+}^C correspond to real eigenvalues. Therefore, the system at threshold is in a stationary state with a phase oscillating in time at the frequency (15a). An analogous solution can be found also, when the strict conservation of energy and momentum does not hold. The relevance of this last solution for the parametric system will be discussed in the next section.

We are now in position to solve Eqs. (7) and (9) numerically as a function of the external field amplitude F_{pump} . For a given value of the external field amplitude, we present in Fig. 1 the time dependent solutions for the signal mode population $N_0(t)$, the anomalous correlation $A(t)$ and the quantity $\omega_{\text{int}} |P_{\mathbf{k}}|^2 / \gamma$, which takes the value I at threshold. For simplicity we set $\gamma_0 = \gamma_{2\mathbf{k}} = \gamma$. We have not reported $N_{2\mathbf{k}}(t)$, because it behaves exactly as $N_0(t)$. The above quantities are calculated with a choice of the material parameters corresponding to a GaAs quantum well in a microcavity and with a polariton broadening $\gamma = 0.5$ meV, which is taken to be the same for all polariton modes. The situation of strict momentum and energy conservation is considered. All three quantities saturate for long times to their stationary values denoted by $P_{\mathbf{k}}^{\text{sat}}$, N_0^{sat} , A^{sat} . The pump mode population $N_{\mathbf{k}}(t)$ grows rapidly for short times and

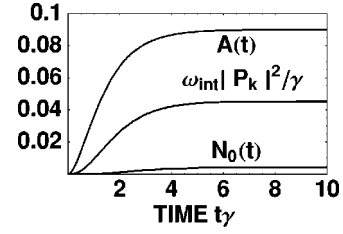


FIG. 1. Plot of the $q=0$ occupation number, the anomalous correlation, and the quantity $\omega_{\text{int}} |P_{\mathbf{k}}|^2 / \gamma$ as a function of time for a pumping field $F_{\text{pump}} = 0.3 F_{\text{threshold}}$, with $F_{\text{threshold}} \equiv \sqrt{\gamma^3 / \omega_{\text{int}}}$. The time unit is $1/\gamma$.

saturates to a value $N_{\mathbf{k}}^{\text{sat}}$ that depends on the external field strength F_{pump} , which has been chosen below the threshold value $F_{\text{threshold}} \equiv \sqrt{\gamma^3 / \omega_{\text{int}}}$. As discussed in Sec. IV, $F_{\text{threshold}}$ corresponds to the threshold in the cw regime. This behavior indicates that during the time evolution an efficient transfer of population between the pump and the signal and idler modes takes place. However, the stationary value $|P_{\mathbf{k}}^{\text{sat}}|^2$, which is obtained from the dynamical equations (7) and (8), is smaller than its threshold value for any value of the amplitude of the external field. This result is consistent with the behavior of $|P_{\mathbf{k}}^{\text{sat}}|^2$ shown in Fig. 2 and indicates that correlations between all three polariton modes are needed, in order to describe the transition to the coherent regime. As shown in Fig. 1, the anomalous correlation $A(t)$ grows rapidly and follows the growth of the pump mode $P_{\mathbf{k}}(t)$ for short times. This behavior originates in the presence of the source term proportional to $|P_{\mathbf{k}}(t)|^2$ in Eq. (9b). Below threshold, the value of the anomalous correlation is much larger than the signal population during the whole time evolution and saturates to a stationary value A^{sat} , which is larger than the one of the mode populations N_0^{sat} , $N_{2\mathbf{k}}^{\text{sat}}$. These characteristics indicate that the build up of the anomalous correlation is the leading process below threshold and that signal and idler remain strongly correlated during the whole time evolution of the system. The growth of the mode populations N_0^{sat} , $N_{2\mathbf{k}}^{\text{sat}}$ is retarded with respect to that of the pump mode $P_{\mathbf{k}}(t)$ and of the anomalous correlation. The peak values of

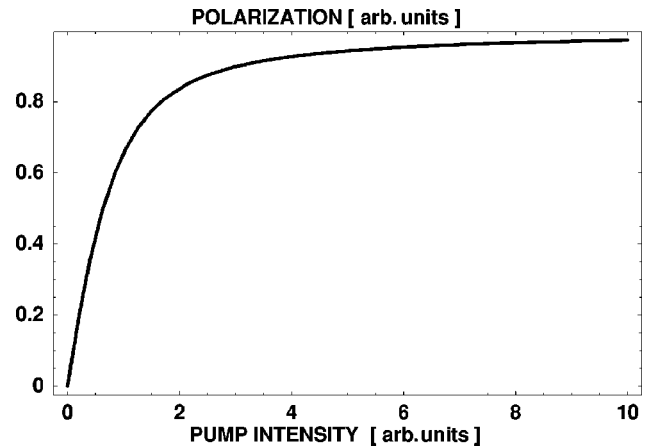


FIG. 2. Polarization of the pumped mode as a function of the external field [Eq. (22)].

the signal and idler populations become important only above threshold. This indicates that the phase correlation, which builds up through the anomalous correlation, is established before the onset of the population through stimulated emission takes place. This result is reminiscent of the time dependent behavior of the signal population with respect to the pump mode, which is observed experimentally in a time resolved pump and probe experiment²³ and confirms the considerations on this subject presented in Ref. 18. The values of the anomalous correlation and of the mode populations become comparable only in the vicinity of the parametric threshold when F_{pump} becomes very large.

IV. STATIONARY SOLUTION

We now calculate the average values of the polarization and the correlations between polariton operators from which experimental quantities such as photoluminescence spectrum and emitted photon statistics are obtained. These quantities are needed in the calculation of the squeezing of the polaritons in the stationary state. To this end, we also have to specify the initial state of the system. For a comparison with experiments, we chose as an initial state either the polariton vacuum or a statistical mixture of n -polariton states.

Let us first consider the equation for the average polarization

$$i \frac{d\langle p_0(t) \rangle}{dt} = [\tilde{\omega}_{\text{LP}}(0) - i\gamma_0] \langle p_0(t) \rangle + \omega_{\text{int}} P_{\mathbf{k}}^2 \langle \hat{p}_{2\mathbf{k}}^+(t) \rangle, \quad (16a)$$

$$i \frac{d\langle \hat{p}_{2\mathbf{k}}^+(t) \rangle}{dt} = -[\tilde{\omega}_{\text{LP}}(2\mathbf{k}) - 2\omega_{\text{pump}} + i\gamma_{2\mathbf{k}}] \langle \hat{p}_{2\mathbf{k}}^+(t) \rangle - \omega_{\text{int}} P_{\mathbf{k}}^{*2} \langle p_0(t) \rangle. \quad (16b)$$

As already mentioned, the amplitude of the pumped mode $|P_{\mathbf{k}}|$ in Eq. (16) is a time independent parameter related to the outside field F_{pump} through the stationary equation (11). The eigenfrequencies of Eq. (16) are given by Eq. (12); these homogenous linear equations have trivial solutions below threshold (i.e., $|P_{\mathbf{k}}|^4 < \gamma_0 \gamma_{2\mathbf{k}} / \omega_{\text{int}}^2$), for the initial states mentioned above. At threshold, the equations show a nontrivial solution oscillating in time and independent on the initial condition. The oscillating frequency is the solution of the compatibility condition obtained from Eq. (16)

$$[\omega - \tilde{\omega}_{\text{LP}}(0) + i\gamma_0][\omega + \tilde{\omega}_{\text{LP}}(2\mathbf{k}) - 2\omega_{\text{pump}} + i\gamma_{2\mathbf{k}}] + \omega_{\text{int}}^2 |P_{\mathbf{k}}|^4 = 0, \quad (17)$$

where $\omega_{\text{int}}^2 |P_{\mathbf{k}}|^4$ takes its threshold value. Therefore, we conclude that at threshold a new state of the system arises, which is characterized by a macroscopic polarization for both, the signal and the idler modes. When energy and momentum are conserved, the solution of Eq. (17) coincides with Eq. (15a) of the previous section. The presence of a macroscopic polarization indicates that a cooperative state has been built up in the system. An analogous result has been derived in Ref. 24 in the framework of a classical three-wave model. This feature has been observed experimentally.⁶ Some characteristics of the behavior of the system above the parametric threshold are discussed in Refs. 19, 20.

We now investigate the behavior of the system below threshold. In this regime, as indicated above the polarization vanishes. The simplest nonvanishing quantities below threshold are the two mode correlations $N_0(t)$, $N_{2\mathbf{k}}(t)$ and the anomalous correlation $A(t)$ introduced in Sec. III. In order to obtain information on the dynamical behavior in the vicinity of the stationary pump mode \mathbf{k} , we evaluate these quantities from the analytical solution of Eqs. (8), where $P_{\mathbf{k}}$ has his stationary value $P_{\mathbf{k}}^{\text{sat}}$. We first evaluate the anomalous correlation $A(t)$ below threshold

$$A(t) = \frac{-\omega_{\text{int}} P_{\mathbf{k}}^2}{(\omega_+ - \omega_-)(\omega_+^C - \omega_-^C)} \times \left\{ \Delta_{2\mathbf{k}}^+ (e^{-it(\omega_+ + \omega_+^C)} - e^{-it(\omega_+ + \omega_-^C)}) \langle 0 | p_0(0) p_0^+(0) | 0 \rangle - \Delta_{2\mathbf{k}}^- (e^{-it(\omega_- + \omega_+^C)} - e^{-it(\omega_- + \omega_-^C)}) \right. \\ \times \langle 0 | p_0(0) p_0^+(0) | 0 \rangle + 2\gamma_0 i \left[\frac{\Delta_{2\mathbf{k}}^+}{(\omega_+ + \omega_+^C)} (e^{-it(\omega_+ + \omega_+^C)} - 1) - \frac{\Delta_{2\mathbf{k}}^+}{(\omega_+ + \omega_-^C)} (e^{-it(\omega_+ + \omega_-^C)} - 1) \right] \\ \left. + 2\gamma_0 i \left[\frac{-\Delta_{2\mathbf{k}}^-}{(\omega_- + \omega_+^C)} (e^{-it(\omega_- + \omega_+^C)} - 1) + \frac{\Delta_{2\mathbf{k}}^-}{(\omega_- + \omega_-^C)} (e^{-it(\omega_- + \omega_-^C)} - 1) \right] \right\}, \quad (18)$$

where $\Delta_{2\mathbf{k}}^\pm = 1/2[\omega_T - i\gamma_S \pm \sqrt{\Lambda}]$ and $\gamma_S = \gamma_{2\mathbf{k}} - \gamma_0$. In Eq. (18), the first two terms in the curly brackets arises from the quantum fluctuation $\langle 0 | p_0(0) p_0^+(0) | 0 \rangle$ in the initial state, which is taken in our case as the polariton vacuum state. The other terms in the curly brackets arise from the correlation of the Langevin forces.

Below threshold, in the limit of infinite time the stationary solution for the anomalous correlation reads

$$\lim_{t \rightarrow \infty} A(t) = -i \frac{(\gamma_T - i\omega_T) \omega_{\text{int}} P_{\mathbf{k}}^2}{\omega_T^2 + \gamma_T^2 - \omega_{\text{int}}^2 |P_{\mathbf{k}}|^4 \gamma_T^2 / \gamma_0 \gamma_{2\mathbf{k}}}. \quad (19)$$

When the threshold values of $P_{\mathbf{k}}$ is inserted in Eq. (18), $A(t)$ becomes

$$A^{\text{threshold}}(t) = \frac{\omega_{\text{int}} P_{\mathbf{k}}^2}{\gamma_T} \times \left\{ \left[\Delta_{2\mathbf{k}}^+(1 - e^{-t\gamma_T}) - \Delta_{2\mathbf{k}}^-(e^{-t\gamma_T} - e^{-2t\gamma_T}) \right] + 2\gamma_0 \left[\Delta_{2\mathbf{k}}^+ t - \frac{\Delta_{2\mathbf{k}}^+}{\gamma_T} (e^{-t\gamma_T} - 1) \right] + 2\gamma_0 \left[\frac{\Delta_{2\mathbf{k}}^-}{\gamma_T} (e^{-t\gamma_T} - 1) - \frac{\Delta_{2\mathbf{k}}^-}{2\gamma_T} (e^{-2t\gamma_T} - 1) \right] \right\}. \quad (20a)$$

$A^{\text{threshold}}(t)$ diverges linearly for large t . This indicates that at threshold this solution becomes unstable, because the contribution of the fluctuations grows in time. This behavior is characteristic of a system undergoing a symmetry breaking transition. Therefore, at threshold the stationary solution (19) for $A(t)$ is meaningless because the state of the system has intrinsically changed and a macroscopic polarization appears, as indicated by Eqs. (16) and (18). However, there exists an explicit expression for A at threshold and for exact momentum and energy conservation, which is found directly from Eqs. (11) and (19). In this regime the stationary anomalous correlation at threshold is

$$|A_{\text{stat}}^{\text{threshold}}| = \frac{1}{2} \sqrt{\frac{\omega_{\text{int}}}{\gamma}} \left(\frac{|F_{\text{pump}}(0)|}{\gamma} - \sqrt{\frac{\gamma}{\omega_{\text{int}}}} \right). \quad (20b)$$

Here it is assumed for simplicity that all polariton modes have the same width. It is evident that in this case the anomalous correlation is completely determined by the external field amplitude. For $F_{\text{pump}}(0)/\gamma < \sqrt{\gamma/\omega_{\text{int}}}$, i.e., below the parametric threshold, the modulus of the anomalous correlation becomes negative and thus meaningless. In Ref. 17, Eqs. (18) are solved together with Eq. (11) in which the factorization $\langle p_0 p_{2\mathbf{k}} \rangle = \langle p_0 \rangle \langle p_{2\mathbf{k}} \rangle$ is performed. The expression for this factorized form of the anomalous correlation coincides with the one given above. This shows that at threshold the anomalous correlation factorizes and the system is indeed in a coherent state.

We now evaluate the stationary occupation number of the signal and idler modes, which read

$$N_0^{\text{sat}} = \frac{\gamma_T}{\gamma_0} \frac{\omega_{\text{int}}^2 |P_{\mathbf{k}}|^4}{\gamma_T^2 + \omega_T^2 - \omega_{\text{int}}^2 |P_{\mathbf{k}}|^4 \gamma_T / \gamma_0 \gamma_{2\mathbf{k}}}, \quad (21a)$$

$$N_{2\mathbf{k}}^{\text{sat}} = \frac{\gamma_0}{\gamma_{2\mathbf{k}}} N_0^{\text{sat}}. \quad (21b)$$

Notice that these quantities are smaller than 1 but become large at threshold thus indicating that a macroscopic occupation of these modes will take place above threshold. This behavior is consistent with the results of the dynamical calculations discussed in Sec. III. The approximations used here are consistently valid when N_0^{sat} and $N_{2\mathbf{k}}^{\text{sat}}$ are less than or of order of 1.

Until now, $P_{\mathbf{k}}$ has been considered as a system parameter. However, this quantity is related to the amplitude of the ex-

ternal source fields through Eq. (11). After having calculated $A(t)$ explicitly, we can discuss the solution of Eq. (11) in detail. Introducing Eq. (19) into Eq. (11) and choosing $\omega_T = 0$ and the external field to be real, we obtain

$$|P_{\mathbf{k}}| \gamma_{\mathbf{k}} + \frac{2\omega_{\text{int}}^2 |P_{\mathbf{k}}|^3}{\gamma_T - \omega_{\text{int}}^2 \gamma_T |P_{\mathbf{k}}|^4 / \gamma_{2\mathbf{k}} \gamma_0} = F_{\text{pump}}. \quad (22)$$

The solution of Eq. (22) is a two-valued function consisting of two branches. The upper branch asymptotically approaches the threshold value of $P_{\mathbf{k}}$ from above and for negative values of F_{pump} whereas the lower branch approaches asymptotically the same value for $P_{\mathbf{k}}$ from below. The upper branch corresponds to values of $P_{\mathbf{k}}$, for which the solutions of Eq. (8) become unstable and the polariton numbers N_0 and $N_{2\mathbf{k}}$ become negative. Equation (22) is solved numerically for the lower branch and its behavior is presented in Fig. 2 in normalized units. In the lower branch the pump polariton amplitude $P_{\mathbf{k}}$ grows linearly with the external field amplitude for a small external field. For larger values of the external field the pump polariton amplitude saturates and approaches asymptotically to a value of $P_{\mathbf{k}}$ that corresponds to the threshold and is independent of F_{pump} . Finally, we notice that the relation (22) allows us to fix the pump mode population $N_{\mathbf{k}} = |P_{\mathbf{k}}|^2$ for a given external excitation and thus to determine the realistic strength of the coupling in Eq. (8). Indeed, the anomalous correlation (19) and the populations (21) as functions of the external field diverge in the unphysical asymptotic limit corresponding to $F_{\text{pump}} \rightarrow \infty$.

V. POLARITON STATISTICS AND SQUEEZING

We are now able to calculate the statistics of the amplified polaritons in the Langevin equations approach and in the stationary regime. We remark that a different approach than the one pursued in this paper consists in evaluating the polariton statistics from the Glauber quasiprobability distribution P . This approach will be discussed elsewhere. The quantity, which is accessible in experiments, is the photon field filtered through the microcavity. This field is related to the polariton amplitude inside the microcavity. The relation between the polariton field inside the microcavity and the field outside the cavity is obtained through the quasimode approach. It reads²

$$\alpha_{\mathbf{q},\Omega}(t) = \alpha_{\mathbf{q},\Omega}(0) e^{-i\Omega t} - i \int_{-\infty}^t dt' \nu(\Omega) C_{\mathbf{q}} P_{\mathbf{q}}(t') e^{-i\Omega(t-t')}. \quad (23)$$

We remember that \mathbf{q} is the in-plane wave vector of the field which in our model is fixed to have the values $\mathbf{q} = 0, \mathbf{k}, 2\mathbf{k}$. The photon field is measured through a detector, and hence averaged in frequency. Therefore, it is useful to introduce the averaged field operators

$$\hat{\alpha}_{\mathbf{q}}(t) = \frac{1}{2\pi} \int_{-\infty}^{\infty} d\Omega \alpha_{\mathbf{q},\Omega}(t). \quad (24a)$$

The corresponding relation between these new operators and the polariton amplitudes reads

$$\hat{\alpha}_{\mathbf{q}}(t) = \frac{1}{2\pi} \int_{-\infty}^{\infty} d\Omega \alpha_{\mathbf{q},\Omega}(0) e^{-i\Omega t} - i\nu C_{\mathbf{q}} p_{\mathbf{q}}(t). \quad (24b)$$

We once more stress the fact that through the relation (24b) the polariton field becomes a measurable quantity in contrast to what happens in the bulk case. This is very important when discussing the statistical properties of polaritons, which can be retrieved from the photon statistics through Eq. (24).

The statistics of the system is characterized through the higher equal time correlations of polariton amplitudes. In particular, we have calculated correlations involving four operators. Correlations involving only one-mode operators show Gaussian properties of the distribution viz.

$$\langle p_0^+ p_0^+ p_0 p_0 \rangle = 2 \langle p_0^+ p_0 \rangle^2 = 2N_0^{\text{sat}}, \quad (25a)$$

$$\langle p_{2\mathbf{k}}^+ p_{2\mathbf{k}}^+ p_{2\mathbf{k}} p_{2\mathbf{k}} \rangle = 2 \langle p_{2\mathbf{k}}^+ p_{2\mathbf{k}} \rangle^2 = 2N_{2\mathbf{k}}^{\text{sat}}. \quad (25b)$$

These correlations can be measured in a standard photon-counting experiment in which only the signal or the idler mode is observed. Correlations involving both modes are non-Gaussian

$$\langle p_0 p_{2\mathbf{k}} p_0 p_{2\mathbf{k}} \rangle = \langle p_0 p_{2\mathbf{k}} \rangle^2 = A^{\text{sat}^2}. \quad (26)$$

From these results we conclude that the field statistics and hence the Glauber quasiprobability distribution will not be standard. From the above results, it is clear that the interesting quantities to be measured are the mixed signal-idler modes. The measurement of these quantities is not straightforward because signal and idler modes are separated in space with an angular separation of about 30° in the experimental setup considered in Ref. 4. Furthermore, the intensity of the field originating in the idler mode is much smaller than that of the signal as a consequence of the small photonic component of the idler. In order to measure mixed moments one has to generate new field amplitude resulting from the superposition of the signal and idler fields. Collecting both the emitted modes by a lens or using mirrors can achieve this goal.

As a last point we evaluate the squeezing of the microcavity polaritons. Nonlinearly interacting microcavity polaritons are good candidates as sources of squeezing. In order to evaluate squeezing we introduce the squeezing operators d_1 and d_2

$$\langle d_1^2 \rangle = \frac{1}{8} \langle [e^{i\theta}(p_0 + p_{2\mathbf{k}}) + e^{-i\theta}(p_0^+ + p_{2\mathbf{k}}^+)] \rangle^2 \quad (27a)$$

and

$$\langle d_2^2 \rangle = -\frac{1}{8} \langle [e^{i\theta}(p_0 + p_{2\mathbf{k}}) - e^{-i\theta}(p_0^+ + p_{2\mathbf{k}}^+)] \rangle^2. \quad (27b)$$

The squeezing will be discussed at resonance $\omega_T = 0$ where the gain of the parametric process is maximum. The amount of squeezing depends on the phase difference between pumped mode $P_{\mathbf{k}} = |P_{\mathbf{k}}| e^{-i\phi}$ and external reference θ . Setting furthermore $\gamma_0 = \gamma_{2\mathbf{k}} = \gamma$ we obtain

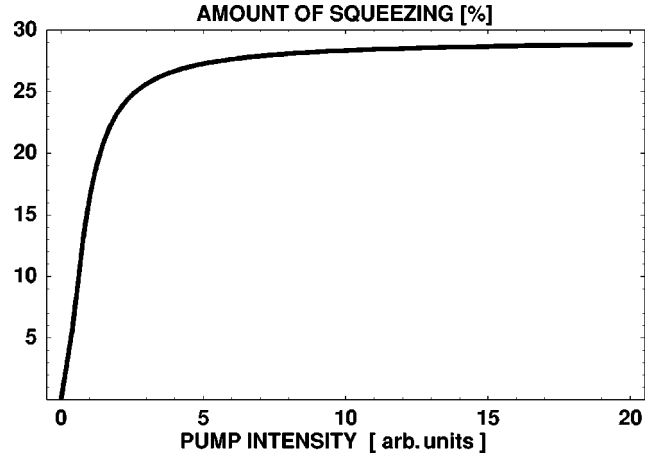


FIG. 3. Amount of squeezing s in percent as a function of the external field.

$$\langle d_{1/2}^2 \rangle = \frac{1/4}{1 - \omega_{\text{int}}^2 |P_{\mathbf{k}}|^4 / \gamma^2} [1 \pm \omega_{\text{int}} |P_{\mathbf{k}}|^2 \sin(\psi) / \gamma] \quad (28)$$

with $\psi = 2(\phi - \theta)$

Near threshold, e.g., $\omega_{\text{int}}^2 |P_{\mathbf{k}}|^4 / \gamma_0 \gamma_{2\mathbf{k}} \approx 1$ and for $\psi = \pi/2$

$$\langle d_1^2 \rangle = \frac{1/4}{1 - \omega_{\text{int}} |P_{\mathbf{k}}|^2 / \gamma} \Rightarrow \infty, \quad (29a)$$

$$\langle d_2^2 \rangle = \frac{1/4}{1 + \omega_{\text{int}} |P_{\mathbf{k}}|^2 / \gamma} \Rightarrow \frac{1}{8}, \quad (29b)$$

and

$$\langle d_1^2 \rangle \langle d_2^2 \rangle > \frac{1}{16}. \quad (29c)$$

Therefore, a non-negligible amount of squeezing is found in the d_2 amplitude only. The amount of squeezing of the outgoing photons may be obtained using the relation (24). In Fig. 3 we plot the squeezing in percent $s = 100(1 - 2\sqrt{\Delta d_2^2})$ as a function of the pump intensity. We notice, that the squeezing saturates at 30% for sufficient large pump intensity. The expression for the spectrum of squeezing, which is also an interesting measurable quantity, is not presented here. Its explicit expression is cumbersome and not very appealing. In fact, it contains a large number of terms, because correlations, which vanish in the stationary regime, also appear. We shall present the calculation for the spectrum of squeezing in the simpler model discussed in the next section.

The feasibility of an experiment in which anomalous correlations and squeezing are measured is related to the magnitude of the wave vector difference between signal and idler. In fact when the idler polariton is mostly excitonlike, the intensity of its emitted field is very small because its photon component expressed through the Hopfield coefficient $C_{2\mathbf{k}}$ in Eq. (24b) is small. This makes the measurement of the anomalous correlations and therefore of the squeezing very difficult. The wave vector difference between idler and signal and thus the ratio of the intensities of the signal and

idler fields may be varied by a convenient choice of the position of the pump mode on the polariton dispersion. When this position is very close to the signal mode at $\mathbf{q}=0$, the three modes are nearly degenerated and the intensities of the emitted fields associated with signal and idler become comparable. The drawback of this configuration is that the very intense pump signal is not easily filtered out because it nearly coincides with the signal and the idler. Although squeezing has not yet been measured, experiments in the above configuration have already been successfully performed.²⁵ In the next section we discuss a simplified model of a parametric system, which may be used to describe the experiments of Messin *et al.*²⁰

VI. THE DEGENERATE PARAMETRIC MODEL

As indicated in the previous section, squeezing is more easily observed when the wave vectors of pump, signal, and idler modes are almost equal. The three-mode amplifier becomes in this case a one-mode system, which is known in the literature as the degenerate parametric amplifier. This model has played a very important role in quantum optics, because it is the simplest model, in which effects such as bistability, amplification, and transition between different operation regimes can be studied.^{9,17,26,27} Furthermore, squeezing has been introduced and extensively studied in this model and the first measurements of the squeezing effect were performed in a degenerate parametric system.²⁸ It is expected that polariton squeezing will also be observable in this configuration. This establishes a link between quantum optics and the physics of polaritons, which may have interesting consequences. In the degenerate case the Hamiltonian (1) has the simpler form

$$H = \hbar \omega_{\text{LP}}(0) p_0^+ p_0 + \hbar \omega_{\text{int}} p_0^{+2} p_0^2 + \hbar F_{\text{pump}} \exp[i \omega_{\text{pump}} t] p_0^+ + \text{H.c.} \quad (30)$$

As already mentioned, the degenerate parametric amplifier has been discussed in great detail in quantum optics (see, e.g., Refs. 26, 27). We summarize some of its characteristics here. The equation of motion for $\hat{p}_0(t)$ is obtained from Eq. (6c) by setting $k=0$. In a first approximation, the external field $F_{\text{pump}}(0)$ forces the system in a coherent state such that the expectation values of the product of polariton operators factorize into products of the expectation values of the polariton amplitudes such as, e.g., $\langle \hat{p}_0^+ \hat{p}_0 \hat{p}_0 \rangle = \langle \hat{p}_0^+ \rangle \langle \hat{p}_0 \rangle \langle \hat{p}_0 \rangle$. In this approximation the stationary solution $\langle \hat{p}_0 \rangle^{\text{stat}}$ for the polariton amplitude is found and shows a bistable behavior in function of the external laser field. Bistability sets in when the detuning between pump and polariton frequencies is negative and its modulus is larger than $\sqrt{3} \gamma_0$.²⁷ We now define the operator

$$\mathbf{P}(t) = \hat{p}_0(t) - \langle \hat{p}_0 \rangle^{\text{stat}} \quad (31)$$

which describes the departure from the stationary state $\langle \hat{p}_0 \rangle^{\text{stat}}$ and allows us to discuss the statistical properties of the system and in particular the squeezing phenomena around the stationary solution. Introducing Eq. (31) into the

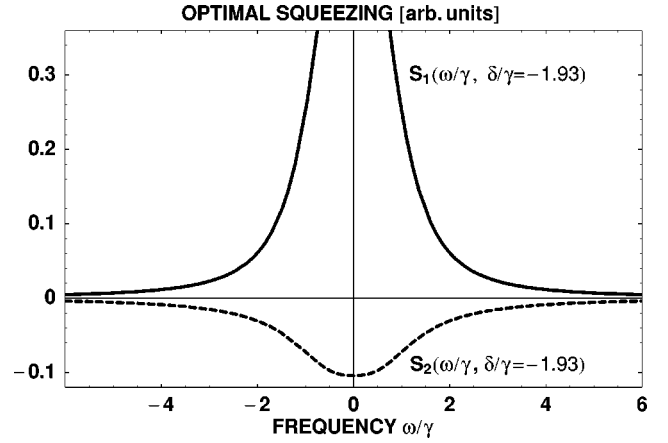


FIG. 4. Optimal spectral squeezing for the degenerate polariton parametric oscillator as a function of the normalized frequency ω/γ for a detuning $\delta = -1.93\gamma$ and an external field $F_{\text{pump}} = 1.58F_{\text{threshold}}$. The quantity $S_1(\omega/\gamma, \delta/\gamma = -1.93)$ has its maximum value 0.628 for $\omega = 0$.

equation of motion for $\hat{p}_0(t)$ and linearizing the resulting equation with respect to $\mathbf{P}(t)$ we obtain

$$i \frac{d}{dt} \mathbf{P}(t) = [\hat{\omega}(0) - \omega_{\text{pump}} - i \gamma_0] \mathbf{P}(t) + 2 \omega_{\text{int}} \mathbf{P}^+(t) (\langle \hat{p}_0 \rangle^{\text{stat}})^2 + \mathbf{F}_0(t) e^{i \omega_{\text{pump}} t}, \quad (32a)$$

where

$$\hat{\omega}(0) = \omega_{\text{LP}}(0) + 4 \omega_{\text{int}} |\langle \hat{p}_0 \rangle^{\text{stat}}|^2. \quad (32b)$$

The time evolution of the operator $\mathbf{P}(t)$ has the same characteristics as that of the signal and idler modes in the non-degenerate case. It decays exponentially and is therefore stable for

$$\gamma_0 \geq \left\{ -[\hat{\omega}(0) - \omega_{\text{pump}}]^2 + 4 \omega_{\text{int}}^2 |\langle \hat{p}_0 \rangle^{\text{stat}}|^4 \right\}^{1/2} \quad (33)$$

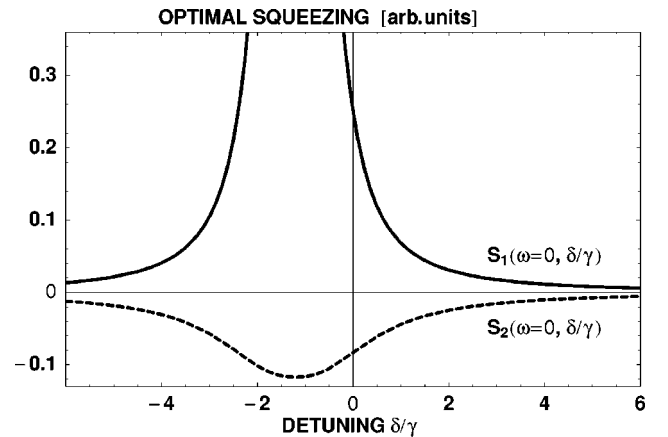


FIG. 5. Optimal spectral squeezing for zero frequency and as a function of the normalized detuning $\delta = (\omega_{\text{LP}}(0) - \omega_{\text{pump}})/\gamma$ for an external field $F_{\text{pump}} = 1.58F_{\text{threshold}}$. The quantity $S_1(\omega = 0, \delta/\gamma)$ has its maximum value 1.875 for $\delta/\gamma = -1.2$.

and is unstable in the opposite case. The equal sign defines the stability limit. The calculation of the relevant statistical features of the model follows the same lines already discussed for the nondegenerate model. Here we discuss in detail the spectral squeezing, which we did not present in the previous section. In analogy to Eq. (27), we introduce for the degenerate case the operators

$$\hat{d}_1(\omega) = \frac{1}{2} [e^{i\theta} \hat{\mathbf{P}}(\omega) + e^{-i\theta} \hat{\mathbf{P}}^+(\omega)] \quad (34a)$$

and

$$\hat{d}_2(\omega) = -\frac{1}{2i} [e^{i\theta} \hat{\mathbf{P}}(\omega) - e^{-i\theta} \hat{\mathbf{P}}^+(\omega)], \quad (34b)$$

where $\hat{\mathbf{P}}(\omega)$ is the Fourier transform of $\mathbf{P}(t)$.

The quantity accessible in most squeezing experiments is the spectrum of squeezing, defined in terms of Eq. (34) by the normal ordered combination^{26,27}

$$S_1(\omega) = \langle : \hat{d}_1(\omega) d_1(t=0) : + : d_1(t=0) \hat{d}_1(-\omega) : \rangle \quad (35a)$$

and

$$S_2(\omega) = \langle : \hat{d}_2(\omega) d_2(t=0) : + : d_2(t=0) \hat{d}_2(-\omega) : \rangle. \quad (35b)$$

The angle θ is the phase of the coherent oscillator used in homodyne detection. It is important to determine the value of θ , for which the expected squeezing will be optimal. For a given value of the frequency $\omega = \omega_0$, the phase is chosen²⁶ such that

$$e^{i\theta} = \frac{\langle \hat{\mathbf{P}}(\omega_0) \mathbf{P}(t=0) \rangle + \langle \mathbf{P}(t=0) \hat{\mathbf{P}}(-\omega_0) \rangle}{|\langle \hat{\mathbf{P}}(\omega_0) \mathbf{P}(t=0) \rangle + \langle \mathbf{P}(t=0) \hat{\mathbf{P}}(-\omega_0) \rangle|}. \quad (36)$$

The explicit expressions for the squeezing spectrum and for the optimal squeezing may be found in the literature.^{26,29} In Fig. 4 and in Fig. 5 we present results for the optimal squeezing evaluated for $\omega_0 = 0$ and for $F_{\text{pump}} = 0.3\gamma$. In Fig. 4 the spectrum of squeezing is presented for a normalized detuning of $\delta = -1.93$, which is slightly smaller than the threshold value $\delta = -\sqrt{3}$ for the bistability to appear. In this case the maximum squeezing with the value $1/8$, appears in S_2 and is attained for $\omega = 0$. The maximum value of the squeezing found here corresponds to the maximum value of the squeezing that is obtained in a double-sided cavity. In Fig. 5 the same quantity is plotted as a function of the detuning and for $\omega = 0$. In this case the maximum value of the squeezing is found for a normalized detuning of $\delta \approx -1.3$. As the external field approaches the threshold value $F_{\text{pump}} = 0.5\gamma$, the maximum value of the squeezing drifts towards a larger negative detuning.

VII. CONCLUSIONS AND OUTLOOK

In conclusion, in this paper we have discussed the dynamical behavior of interacting polaritons in a microcavity in the framework of a three mode model^{17,18} under the assumption that the pump mode can be factorized out of correlation involving the three polariton modes. We have presented a detailed discussion of the behavior in time of the anomalous correlation and of the modes occupation numbers, showing the importance of the anomalous correlation in the dynamics of the system. In particular we discuss the approach of the polariton occupation numbers and of the anomalous correlation to their stationary values and show that the population transfer from the pump to the idler and signal modes through the anomalous correlation dominates the dynamics. The stationary solutions are presented for a choice of the external field below threshold and at the threshold. We show that at threshold the anomalous correlation factorizes into the product of the signal and idler modes amplitudes as it is expected for a macroscopically occupied state.^{17,18,24} Furthermore, we have introduced the statistical properties of the polariton modes and thus of the emitted field showing a non-Gaussian behavior. In particular we show that a non-negligible amount of squeezing is present in the correlation between signal and idler fields. Finally the model has been adapted to possible experimental configurations²⁵ in which idler and signal almost coincide and the optimal squeezing spectrum has been evaluated as a function of the frequency and as a function of the detuning for a given frequency.

We conclude by giving an outlook on the open problems in this context. The model discussed in this paper represents a useful but strongly simplified description of the parametric system. As we have already mentioned, the three-mode description is well justified below the parametric threshold, but represents an oversimplification as the parametric threshold is reached and fails above threshold. Therefore, a many mode description^{6,19} of the amplification process will be necessary. In our discussion we have considered the fluctuation induced by the losses from the microcavity as being responsible for the polariton broadening. Although the experiments are performed at very low temperatures, the influence of the exciton-phonon interaction on the parametric process should be considered. Furthermore the exciton-phonon interaction becomes essential when effects such as the gain dependence on temperature³⁰ has to be described. Moreover, two other effects can affect the squeezing properties, namely, the coupling to an incoherent bath of excitons and the residual polariton-polariton interaction beyond the mean field limit. More refined treatments are under current investigation.³¹

ACKNOWLEDGMENTS

We acknowledge illuminating discussions with E. Giacobino, J.-P. Karr, S. Kundermann, J.-L. Staehli, and M. Saba.

- *Permanent address: Laboratoire de Physique de la Matière Condensée, Ecole Normale Supérieure, 24 rue Lhomond, F-75005 Paris, France.
- ¹C. Weisbuch, M. Nishioka, A. Ishikawa, and Y. Arakawa, *Phys. Rev. Lett.* **69**, 3314 (1992).
 - ²V. Savona, C. Piermarocchi, A. Quattropani, P. Schwendimann, and F. Tassone, *Phase Transitions* **68**, 169 (1999).
 - ³R. Houdré, C. Weisbuch, R. P. Stanley, U. Oesterle, and M. Illegems, *Phys. Rev. Lett.* **73**, 2043 (1994).
 - ⁴P. G. Savvidis, J. J. Baumberg, R. M. Stevenson, M. S. Skolnick, D. M. Whittaker, and J. S. Roberts, *Phys. Rev. Lett.* **84**, 1547 (2000).
 - ⁵R. Houdré, C. Weisbuch, R. P. Stanley, U. Oesterle, and M. Illegems, *Phys. Rev. Lett.* **85**, 2793 (2000).
 - ⁶P. G. Savvidis, C. Ciuti, J. J. Baumberg, M. S. Skolnick, D. M. Whittaker, and J. S. Roberts, *Phys. Rev. B* **64**, 075311 (2001).
 - ⁷R. Huang, F. Tassone, and Y. Yamamoto, *Phys. Rev. B* **61**, R7854 (2000).
 - ⁸R. M. Stevenson, V. N. Astratov, M. S. Skolnick, D. M. Whittaker, M. Emam Ismail, A. I. Tartakovskii, P. G. Savvidis, J. J. Baumberg, and J. S. Roberts, *Phys. Rev. Lett.* **85**, 3680 (2000).
 - ⁹See, e.g., *Nonclassical Effects in Quantum Optics*, edited by P. Meystre and D. F. Walls (American Institute of Physics, Woodbury, 1991).
 - ¹⁰P. Schwendimann and A. Quattropani, *Nuovo Cimento D* **15**, 1421 (1993).
 - ¹¹M. Artoni and J. L. Birman, *Phys. Rev. B* **44**, 3736 (1991).
 - ¹²Z. Hradil, A. Quattropani, V. Savona, and P. Schwendimann, *J. Phys. IV* **3**, 393 (1993).
 - ¹³S. Savasta and R. Girlanda, *Phys. Rev. Lett.* **77**, 4736 (1996).
 - ¹⁴S. Savasta, R. Girlanda, and G. Martino, *Phys. Status Solidi A* **164**, 85 (1997).
 - ¹⁵M. Kira, F. Jahnke, and S. W. Koch, *Phys. Rev. Lett.* **82**, 3544 (1999).
 - ¹⁶R. Shimano, Yu P. Svirko, A. Mysyrowicz, and M. Kuwata-Gonokami, *Phys. Rev. Lett.* **89**, 233601 (2002).
 - ¹⁷C. Ciuti, P. Schwendimann, B. Deveaud, and A. Quattropani, *Phys. Rev. B* **62**, R4825 (2000).
 - ¹⁸C. Ciuti, P. Schwendimann, and A. Quattropani, *Phys. Rev. B* **63**, 041303 (2001).
 - ¹⁹C. Ciuti, P. Schwendimann, and A. Quattropani, *Semicond. Sci. Technol.* (to be published).
 - ²⁰C. Ciuti, P. Schwendimann, and A. Quattropani, *Phys. Status Solidi A* **190**, 305 (2002).
 - ²¹J.-Ph. Karr, A. Baas, R. Houdré, and E. Giacobino, *cond-mat/0305106* (unpublished).
 - ²²G. Rochat, C. Ciuti, C. Piermarocchi, V. Savona, A. Quattropani, and P. Schwendimann, *Phys. Rev. B* **61**, 13 856 (2000).
 - ²³M. Saba (private communication).
 - ²⁴D. M. Whittaker, *Phys. Rev. B* **63**, 193305 (2001).
 - ²⁵G. Messin, J.-Ph. Karr, A. Baas, G. Khitrova, R. Houdré, R. P. Stanley, U. Oesterle, and E. Giacobino, *Phys. Rev. Lett.* **87**, 127403 (2001).
 - ²⁶M. J. Collet and D. F. Walls, *Phys. Rev. A* **32**, 2887 (1985).
 - ²⁷F. A. Hopf, P. Meystre, P. D. Drummond, and D. F. Walls, *Opt. Commun.* **31**, 245 (1979).
 - ²⁸R. E. Slusher, L. W. Hollberg, B. Yurke, J. C. Mertz, and J. F. Valley, *Phys. Rev. Lett.* **55**, 2409 (1985).
 - ²⁹G. Messin, J.-Ph. Karr, H. Eleuch, J. M. Courty, and E. Giacobino, *J. Phys.: Condens. Matter* **11**, 6069 (1999).
 - ³⁰M. Saba, C. Ciuti, J. Bloch, V. Thierry-Mieg, R. André, Le Si Dang, S. Kundermann, A. Mura, G. Bongiovanni, J. L. Staehli, and B. Deveaud, *Nature (London)* **414**, 731 (2001).
 - ³¹S. Savasta, O. di Stefano, and R. Girlanda, *Phys. Rev. Lett.* **90**, 096403 (2003).